

# Dynamics of ternary polymer blends: Disordered, ordered and bicontinuous microemulsion phases

Terry L. Morkved,<sup>a</sup> Bryan R. Chapman,<sup>a</sup> Frank S. Bates,<sup>a</sup> Timothy P. Lodge,<sup>a</sup> Petr Stepanek<sup>b</sup> and Kristoffer Almdal<sup>c</sup>

<sup>a</sup> Department of Chemical Engineering & Materials Science and Department of Chemistry, University of Minnesota, Minneapolis, MN 55455-0431, USA

<sup>b</sup> Institute of Macromolecular Chemistry, Czech Academy of Sciences, Prague, Czech Republic

<sup>c</sup> Department of Solid State Physics, Risø National Laboratory, DK-4000 Roskilde, Denmark

Received 24th November 1998

Dynamic light scattering has been used to examine the order parameter fluctuations in ternary homopolymer/homopolymer/block copolymer blends. The chemical system consists of poly(dimethylsiloxane) (PDMS) and poly(ethylene) (PEE) homopolymers of nearly equal molecular volumes, and a nearly symmetric PDMS–PEE diblock copolymer. The phase diagram along the isopleth (*i.e.*, equal volumes of each homopolymer) includes a disordered region at high temperatures that at low temperatures evolves into (a) a swollen lamellar phase in the copolymer-rich region; (b) a phase-separated state when there are only modest amounts of copolymer; (c) a narrow channel of bicontinuous microemulsion for copolymer compositions near where mean-field theory anticipates an isotropic Lifshitz point. Intensity autocorrelation functions for the binary blend are single exponential decays, and the associated correlation length  $\xi$  scales with reduced temperature  $\varepsilon$  in accordance with the Ising universality class (*i.e.*,  $\xi \sim \varepsilon^{-\nu}$ , with  $\nu = 0.63$ ). The addition of copolymer depresses the critical temperature, but also increases the magnitude of  $\nu$ . For compositions within the microemulsion channel  $\xi$  exhibits a clear maximum with decreasing temperature, near the Lifshitz line obtained from the static structure factor. For one particular composition there is a “re-entrant” microemulsion, as the system passes into and then out of the phase-separated region upon cooling. Below the Lifshitz line there is consistent evidence of one or two small amplitude, faster modes in the correlation functions. These modes are also apparent in blends with compositions corresponding to the swollen lamellar phase, and are tentatively attributed to translational diffusion of the copolymer and undulations of the layers.

## Introduction

Multicomponent polymer blends are technologically very important, as they offer relatively direct routes to tailoring physical properties. Owing to the low combinatorial entropy of mixing associated with long chain molecules, most polymer pairs are not miscible. Consequently, it is often advantageous to stabilize a dispersion of one component in another by use of a macromolecular

surfactant, such as a block copolymer. Furthermore, as has recently become apparent, it is possible to utilize copolymers to direct the system to adopt more controlled and varied morphologies,<sup>1–4</sup> such as bicontinuous microemulsions.<sup>5</sup>

Model polymer blends also present attractive systems for studying the basic thermodynamics and dynamics of mixtures, for a variety of reasons.<sup>6</sup> First, the multiple contacts between neighboring molecules and generally weak interactions renders mean-field theory more applicable, and in some cases the phase diagram is almost quantitatively describable by the regular solution (Flory–Huggins) free energy. Second, the thermodynamic state of the system is governed by the dimensionless product  $\chi N$ , where  $\chi$  is the interaction parameter and  $N$  is the degree of polymerization, and both  $\chi$  ( $\sim 1/T$ ) and  $N$  (by controlled synthesis) may be varied systematically. Third, the length and time scales associated with macromolecules are favorable for detailed analysis of *structure*, for example, by small-angle X-ray or neutron scattering or electron microscopy, *dynamics*, for example, by dynamic light scattering and NMR, and *kinetics*.

We have recently demonstrated the formation of bicontinuous polymeric microemulsions in three different chemical systems, utilizing 50 : 50 mixtures of two homopolymers of similar size combined with small amounts of a symmetric diblock copolymer of the same components.<sup>5,7</sup> The microemulsion phase appears as a narrow channel in copolymer concentration, intermediate between a swollen lamellar phase on the copolymer-rich side and a phase-separated mixture on the other. Furthermore, this composition range coincides with the regime where mean-field theory anticipates an isotropic Lifshitz point,<sup>8,9</sup> i.e., a point where disordered, uniformly ordered, and periodically ordered phases meet.<sup>10</sup> Indeed, in one system Lifshitz-like behavior was found to within one degree of the putative Lifshitz point,<sup>11</sup> even though fluctuations are expected to destroy the Lifshitz point in favor of phases such as the bicontinuous microemulsion.

In this paper, we use a dynamic light scattering to explore the dynamics of concentration fluctuations in bicontinuous microemulsions containing poly(dimethylsiloxane) (PDMS), poly(ethylene) (PEE), and a PDMS-PEE diblock copolymer. For comparison purposes, results on the copolymer-rich and copolymer-lean sides of the microemulsion channel are also presented. As far as we are aware, this represents the first study of the dynamic structure factor of any system in the vicinity of an isotropic Lifshitz point, and particularly of a bicontinuous polymeric microemulsion. Some dynamic light scattering measurements on bicontinuous oil/water/surfactant systems have been reported,<sup>12</sup> and considerable attention has been directed to the dynamics of order parameter fluctuations in the vicinity of another Lifshitz point, that occurring in ferroelectric liquid crystals under a magnetic field.<sup>13,14</sup>

## Experimental

### Materials

The polymer samples were all prepared by living anionic polymerization following standard procedures, as described elsewhere.<sup>15</sup> The number average molecular weights determined by NMR were 2130 for poly(dimethylsiloxane) (PDMS), 1710 for poly(ethylene) (PEE), and 10400 for the PDMS-PEE diblock. The composition of the diblock was 52% PDMS by volume. PEE was prepared by catalytic deuteration of the appropriate poly(buta-1,2-diene) precursor. The degree of 1,2-addition was 90% and the extent of hydrogenation >99%, as determined by NMR.

Blends were prepared gravimetrically, and then co-dissolved in pentane and filtered through 0.45  $\mu\text{m}$  filters into de-dusted 5 mm i.d. scattering cells. The pentane was extracted *in vacuo* and the cells were then sealed. Each sample contained equal volumes of PDMS and PEE, and the volume fractions of copolymer were 0, 0.042, 0.071, 0.092, 0.100, and 0.180. Volume fractions were calculated assuming additivity of volumes and densities (measured at room temperature) of 0.954, 0.883, and 0.935 g ml<sup>−1</sup> for PDMS, PEE, and PDMS-PEE, respectively.

### Measurements

Dynamic light scattering measurements were taken on two instruments, one at the University of Minnesota and one at the Institute of Macromolecular Chemistry, as previously described.<sup>16,17</sup>

Each instrument has fully adjustable scattering angle,  $\theta$ , and temperature control to  $\pm 0.1^\circ\text{C}$  from at least 0 to  $200^\circ\text{C}$ . HeNe ( $\lambda_0 = 632.8\text{ nm}$ ) or Ar<sup>+</sup> lasers ( $\lambda_0 = 488.0$  or  $514.5\text{ nm}$ ) were employed. The autocorrelation functions of the scattered light intensity,  $g^{(2)}(q, t)$ , were obtained with multi-tau correlators (Brookhaven BI-9000 at Minnesota and ALV-5000 in Prague) and analyzed either by fitting to a single exponential decay, or by the regularized nonlinear inverse Laplace transformation program REPES.<sup>18,19</sup> REPES is similar to the more familiar inverse Laplace transform routine CONTIN,<sup>20</sup> except that it fits the intensity correlation function  $g^{(2)}(t)$  directly (*i.e.*, instead of taking the square root of  $g^{(2)}$  to generate  $g^{(1)}$ ), and it is possible to preselect a “probability to reject” at which the inversion is calculated.

The viscosity of the sample with homopolymer volume fraction  $\phi_{\text{H}} = 0.900$  was measured on a Rheometric Scientific DSR from 25 to  $150^\circ\text{C}$ . The sample was confined between 25 mm diameter parallel plates, and steady flow was imposed with strain rates between 1 and  $100\text{ s}^{-1}$ . The results were fit to the Williams–Landel–Ferry (WLF) equation<sup>21</sup>

$$\log \frac{\eta}{\eta_r} = \frac{-C_1(T - T_r)}{C_2 + T - T_r} \quad (1)$$

with constants  $C_1 = 3.027$  and  $C_2 = 136.9^\circ\text{C}$  and a reference temperature  $T_r$  of  $80.0^\circ\text{C}$ ;  $\eta_r = 0.131\text{ Pa s}$ . Viscosities for the other compositions were estimated assuming the same  $T$  dependence, and scaling to the appropriate sample weight average molecular weight assuming Rouse dynamics (*i.e.*,  $\eta \sim M$ ).

Small-angle neutron scattering (SANS) measurements were performed either at the 12 m SANS facility at Risø National Laboratory or on the 30 m Exxon/Minnesota/NIST SANS instrument at NIST. Samples were contained in quartz spectrophotometer cells, which were then sealed with a high temperature adhesive. Data were corrected for background, detector response, transmission and incoherent contributions. The intensity obtained on a two-dimensional detector was azimuthally averaged to provide scattering functions  $I(q)$ , where  $q$  is the standard scattering wavevector ( $= 4\pi/\lambda \sin \theta/2$ ).

## Background

### Phase behavior

The complete phase behavior of an A homopolymer/B homopolymer/AB diblock copolymer ternary blend depends on an array of variables: the degrees of polymerization,  $N_{\text{A}}$ ,  $N_{\text{B}}$ , and  $N_{\text{AB}}$ , the composition of the copolymer,  $f_{\text{A}}$ , the volume fractions of the two homopolymers,  $\phi_{\text{A}}$  and  $\phi_{\text{B}}$ , and temperature,  $T$ .<sup>8,9,22–24</sup> We restrict our attention to symmetric systems, *i.e.*, where  $N_{\text{A}} = N_{\text{B}} = N$ ,  $\phi_{\text{A}} = \phi_{\text{B}}$ , and  $f = 1/2$ , and thus the mixtures contain equal amounts of A and B segments. In this case the phase diagram can be displayed as a plot of  $T$  versus  $\phi_{\text{H}}$ , where  $\phi_{\text{H}} = \phi_{\text{A}} + \phi_{\text{B}}$  is the total volume fraction of homopolymer, for a given value of  $N$  and  $\alpha = N/N_{\text{AB}}$ . Furthermore, we consider only the case where  $\alpha < 1$ , for which the (longer) copolymer is effective at compatibilizing the homopolymer blend, and is also capable of forming mesophases.<sup>9</sup> This situation has been considered in detail utilizing mean-field theory (*i.e.*, Flory–Huggins-like for disordered phases and the random phase approximation for the onset of order).<sup>8,9,23,24</sup> The qualitative features of the theory are illustrated in Fig. 1, for the particular case  $\alpha = 0.20$ ; this value is chosen so that the critical temperature ( $T_{\text{c}}$ ) of the binary blend ( $\phi_{\text{H}} = 1$ ) is approximately equal to the order–disorder transition (ODT) temperature for the pure diblock ( $\phi_{\text{H}} = 0$ ). These two temperatures are connected by a  $\lambda$ -line, separating the high  $T$  disordered phase from either a periodically ordered lamellar (LAM) phase at low  $\phi_{\text{H}}$  or two coexisting “uniformly ordered” liquid phases ( $2\phi$ ) at high  $\phi_{\text{H}}$ . The line of (second order) ODTs meets the line of critical points at an isotropic Lifshitz point (LP), a special point where the critical divergence departs continuously from wavevector  $q^* = 0$  to  $q^* > 0$ . The LAM and  $2\phi$  states are separated by an unbinding transition (UT), which extends down from the LP to a region of three-phase coexistence ( $3\phi$ ; one periodically ordered, rich in copolymer, and two uniformly ordered, rich in each homopolymer).

Experimentally one does not anticipate strict adherence to mean-field theory. For example, in a pure blend there is a window of Ising-like behavior close to  $T_{\text{c}}$ ,<sup>17,25–28</sup> although this interval

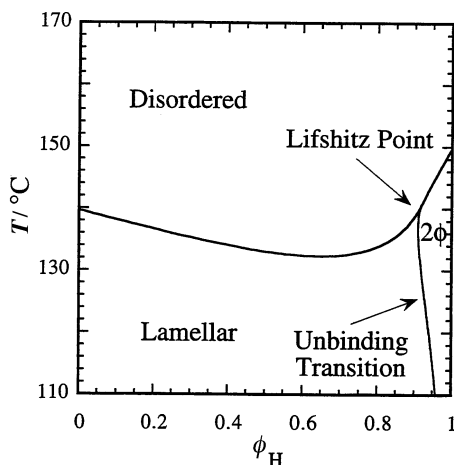


**Fig. 1** Theoretical mean-field phase diagram for a symmetric homopolymer/homopolymer/block copolymer blend with equal volume fractions of each homopolymers,<sup>8</sup> with  $\alpha \approx 0.2$ .  $\phi_H$  is the total volume fraction of homopolymer. The unbinding transition separates the lamellar and two phase ( $2\phi$ ) regions and meets the order–disorder transition and stability lines at an isotropic Lifshitz point.

scales as  $N^{-1}$  and is therefore rather small.<sup>29–31</sup> In the pure diblock the ODT is a fluctuation-induced weakly first-order transition, as anticipated by Brazovskii,<sup>32</sup> Leibler,<sup>33</sup> and Fredrickson and Helfand;<sup>34</sup> these fluctuations are important over a wider  $T$  interval that scales as  $N^{-1/3}$ . The line of ODTs should therefore exhibit a regime of two-phase coexistence, although this is also extremely narrow. The LP is of particular interest, as an isotropic LP has apparently never been observed; isotropic in this sense means that the dimension of space equals the number of dimensions in which the instability occurs. This behavior can be conveniently categorized through the use of a Landau–Ginzburg free energy density with scalar order parameter  $\psi(r)$ :

$$F(\psi) = a_2 \psi^2 + a_4 \psi^4 + a_6 \psi^6 \cdots + c_1 (\nabla \psi)^2 + c_2 (\nabla^2 \psi)^2 + \cdots \quad (2)$$

where the coefficients  $a_2, a_4, a_6 \dots c_1, c_2, \dots$ , etc., are system dependent. At an ordinary critical point  $a_2 = 0$  with all other coefficients positive, and the system passes from a disordered state to a uniformly ordered state with  $q^* = 0$ . At the LP both  $a_2$  and  $c_1$  vanish, and three distinct phases meet: disordered, uniformly ordered ( $a_2 < 0, c_1 > 0$ ) and periodically ordered ( $a_2 < 0, c_1 < 0$ ).

The phase behavior of three nearly symmetric systems with  $\alpha \approx 0.2$  have been reported: polyethylene (PE)/poly(ethylenepropylene) (PEP),<sup>11,35</sup> poly(dimethylsiloxane) (PDMS)/poly(ethylethylene) (PEE),<sup>2,7</sup> and poly(ethyleneoxide) (PEO)/PEE.<sup>7</sup> In all three cases the important departure from mean-field theory is the appearance of a narrow channel of bicontinuous microemulsion ( $\mu$ E) in the vicinity of the predicted UT. This is illustrated in Fig. 2 for PDMS/PEE, the system of interest in this paper. This phenomenon may be qualitatively understood in terms of fluctuations destroying the LAM structure before the periodicity  $d \sim 1/q^*$  diverges. Interestingly, as mentioned in the Introduction a PE/PEP/PE–PEP sample at the Lifshitz composition exhibited critical behavior conforming to that predicted to within 1 °C of the LP.<sup>11</sup> In particular, the concentration fluctuation correlation length,  $\xi$ , scaled as  $(T - T_{LP}/T_{LP})^{-0.25}$ , consistent with the predicted scaling ( $\nu = 1/4$ ) but in contrast to the binary mixture predictions of  $\varepsilon^{-\nu}$  ( $\varepsilon = (T - T_c/T_c)$ ), with  $\nu = 1/2$  (mean-field) or 0.63 (Ising). Thus the microemulsion is created by adding more copolymer, and the fluctuations become dominant abruptly on the copolymer-rich side of the LP. In all three systems the location of the  $\mu$ E channel could therefore have been estimated *a priori* simply on the basis of the predicted LP.<sup>36</sup> In order to visualize the structure of this phase, Fig. 3 presents transmission electron micrographs of the  $\mu$ E phase and neighboring LAM and phase-separated structures in PE/PEP;<sup>11</sup> the crystallization of the PE facilitated freezing-in the structure for staining the amorphous PEP domains.

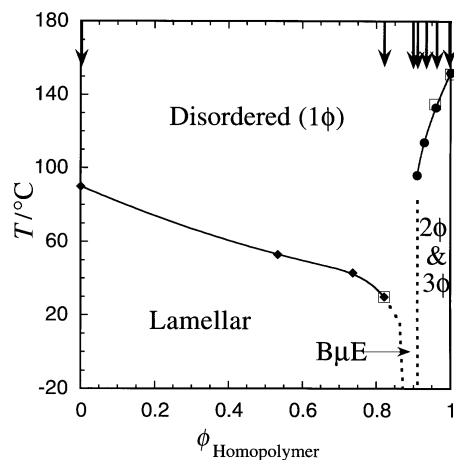


**Fig. 2** Experimental phase diagram for a symmetric PDMS/PEE/PDMS-PEE blend. Four phases are found: disordered, lamellar, bicontinuous microemulsion ( $\mu\text{E}$ ), and phase-separated ( $2\phi$  and  $3\phi$ ). The curves delineate the phase boundaries as measured by light scattering (circles), rheology (diamonds), and SANS (squares). The arrows indicate the blend concentration examined by DLS.

### Dynamics

In this paper we emphasize the dynamic structure factor  $S(q, t)$  of ternary blends, as revealed by dynamic light scattering (DLS). In this instance the range of accessible wavevectors corresponds to length scales considerably larger than the constituent molecules, and one probes the rise and decay

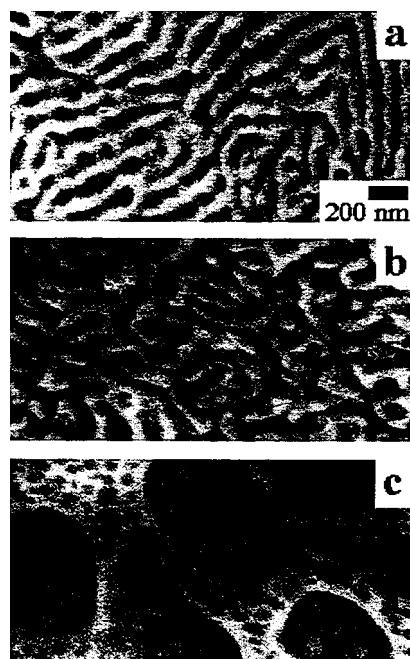


**Fig. 3** Transmission electron micrographs from symmetric PE/PEP/PE-PEP blends.<sup>5</sup> The samples were prepared by annealing at 119 °C followed by a rapid quench below the crystallization temperature. The PEP block was stained by ruthenium tetroxide and appears dark in the micrographs. These images are consistent with (a) fluctuating lamellae, with  $\phi_{\text{H}} = 0.860$ , (b) bicontinuous microemulsion, with  $\phi_{\text{H}} = 0.900$ , and (c) complementary droplet microemulsion in the phase-separated regime, with  $\phi_{\text{H}} = 0.920$ .

of spontaneous collective concentration fluctuations of PEE and PDMS segments. In the case that  $S(q, t)$  is well-described by a single exponential, the decay rate  $\Gamma$  may be written generically as

$$\Gamma = q^2 \frac{A}{S(q)} \quad (3)$$

where  $A$  is an Onsager coefficient (that may depend on  $q$ ) and  $S(q)$  is the static structure factor. However, in an incompressible three-component system one expects the decay of concentration fluctuations to be described by at least two modes, the relative amplitudes and decay rates of which are dependent on various aspects of the system.<sup>37–40</sup>

For binary polymer blends at the critical composition, the results follow eqn. (3) as has been shown for several systems.<sup>17,27</sup> Furthermore, the resulting diffusivity,  $D = A/S$ , follows the Kawasaki–Stokes–Einstein form

$$D = \frac{kT}{6\pi\eta\xi} \quad (4)$$

which defines a dynamic correlation length  $\xi$ . This correlation length exhibits a broad crossover from mean-field ( $\xi \sim \varepsilon^{-1/2}$ ) to Ising scaling ( $\xi \sim \varepsilon^{-0.63}$ ) around a Ginzburg temperature a few degrees above  $T_c$ , just as does the static correlation length determined from  $S(q)$ .<sup>17,27</sup>

The DLS from pure diblock copolymers has proven to be considerably more complex. Theory anticipates a single “internal” mode, with  $\Gamma$  independent of  $q$ , that corresponds to relative motion of the two blocks of one chain.<sup>41,42</sup> This mode has very small amplitude for small block copolymers and can be hard to detect. A second, slower diffusive mode has generally been observed and is now understood as arising from chain-to-chain variations in composition, that allow long-wavelength fluctuations in monomer concentration.<sup>41,43</sup> This “heterogeneity” mode therefore reflects translational diffusion of the chains. Additional modes have also been reported, however, and remain incompletely understood, as has recently been discussed.<sup>16,44</sup>

In a symmetric ternary system it is tempting to postulate two orthogonal modes, one corresponding to fluctuations in total A *versus* total B monomer concentration, and the other to copolymer *versus* total homopolymer concentration. The first mode reduces to the single mode seen in the case of a binary blend, and the second mode should be invisible if the homopolymers are homogeneously mixed and the copolymer is truly symmetric. However, as the segregation of A and B homopolymers increases with decreasing temperature, the motion of the copolymer could become visible against an A-rich or B-rich background.

## Results and discussion

This section is subdivided into three parts, corresponding to the homopolymer-rich side of the  $\mu E$  channel ( $\phi_H > \phi_{LP}$ ), the  $\mu E$  channel, and the copolymer-rich side, respectively. The compositions examined by DLS are all indicated as arrows on the experimental phase diagram in Fig. 2.

### Homopolymer-rich blends

From SANS the critical temperature of the binary blend was determined to be 151.4 ( $\pm 1$ ) °C, by extrapolating the inverse  $q = 0$  intensity *versus*  $1/T$ .<sup>7</sup> (More precisely, it is the stability limit that was determined, because a precise mapping of the binary phase diagram was not performed.) The DLS correlation functions were all very well described by single exponential decays, as illustrated in Fig. 4. Furthermore, the decay rate  $\Gamma$  was proportional to  $q^2$  with zero intercept, as shown in the inset to Fig. 4. The correlation length was extracted *via* eqn. (4), using the measured viscosity of  $T$ . Anticipating Ising-like scaling, the data are plotted in Fig. 5 as  $\xi^{-1/0.63}$  *versus*  $1/T$  for a 20 °C interval above  $T_c$ , the extrapolated value of  $T_c$  coincides well with the SANS value, and the linearity of the data confirms the Ising behavior. The relatively wide interval of non-mean-field response in this case is a consequence of the low molecular weights involved.

Similar DLS experiments and analyses were performed for blends containing 4.2% and 7.1% copolymer, and the decays were all single exponential. The resulting values of  $\xi$  are compared as a function of  $T$  in Fig. 6. The functional form of  $\xi(T)$  is apparently similar, but the magnitudes

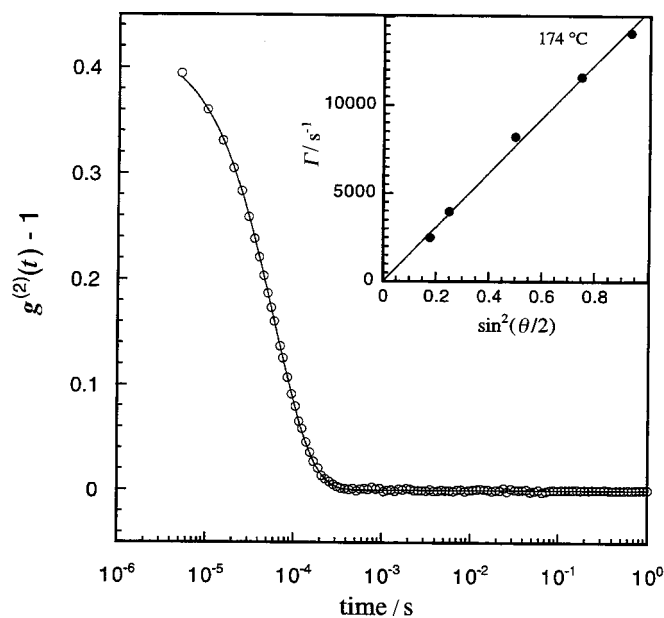


**Fig. 4** Intensity correlation functions,  $g^{(2)}(t)$ , for the symmetric binary PDMS/PEE blend at  $T = 174^\circ\text{C}$  and  $\theta = 90^\circ$ . The angular dependence of the decay rate,  $\Gamma$ , is plotted in the inset and shows diffusive dynamics ( $\Gamma \sim q^2$ ).

decrease significantly with copolymer concentration at fixed  $T$ . This is directly attributable to the reduction in  $T_c$  upon the addition of copolymer. However, it turns out that the functional form of  $\xi(T)$  is not independent of copolymer concentration. For example,  $\xi(T)$  is plotted in the “Ising format” (cf. Fig. 5) for the 7.1% blend in Fig. 7, and clear deviations are apparent as  $T_c$  is approached. Interestingly, the magnitude of the apparent exponent  $\nu$  is becoming larger than 0.63, so this is not a trend toward the mean-field “Lifshitz-like” behavior ( $\nu = 0.25$ ) seen in PE/PEP.<sup>11,45</sup> In that system, mean-field exponents were found essentially all the way down to the phase boundary, both in the blend and with modest amounts of copolymer.<sup>45</sup> Schwahn and coworkers also found with these PDMS/PEE materials that the static correlation length and susceptibility gave exponents that were larger in magnitude than Ising, consistent with our results;

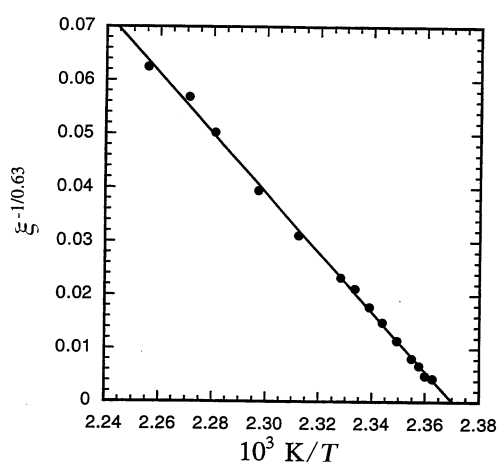


**Fig. 5** Dynamic correlation length  $\xi$  (in nm) raised to the  $-1/0.63$  power as a function of inverse temperature for the symmetric binary PDMS/PEE blend. The linear fit confirms the expected Ising critical behavior.



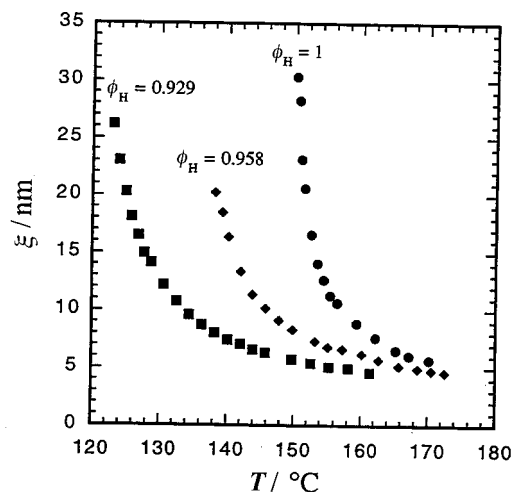


**Fig. 6** Dynamic correlation length  $\xi$  as a function of temperature for three symmetric blends:  $\phi_H = 1$  (circles),  $\phi_H = 0.958$  (diamonds), and  $\phi_H = 0.929$  (squares).

they attributed this phenomenon to the larger upper critical dimension ( $=8$ ) in the ternary system.<sup>2</sup> Physically, one can view this as the presence of copolymer opposing the growth of  $\xi$ , due to the concomitant compression of copolymers at the interface as the amount of interface decreases. Thus, the main effects on the dynamics of adding copolymer are (i) to suppress the stability limit and, therefore, the critical slowing down at a given temperature, and (ii) to change the apparent values of the critical exponents.

#### $\mu$ E channel

For the given value of  $\alpha \approx 0.19$  the mean-field theory predicts that  $\phi_{LP} = 1/(1 + 2\alpha^2) \approx 0.93$ . Accordingly, a sample with slightly less copolymer,  $\phi_H = 0.900$ , was examined in detail with DLS; SANS measurements performed previously established that this composition falls in the  $\mu$ E channel.<sup>7</sup> At all temperatures examined (from 10 to 140 °C) the autocorrelation function was dominated by a single diffusive mode. The associated diffusion coefficient was converted to a

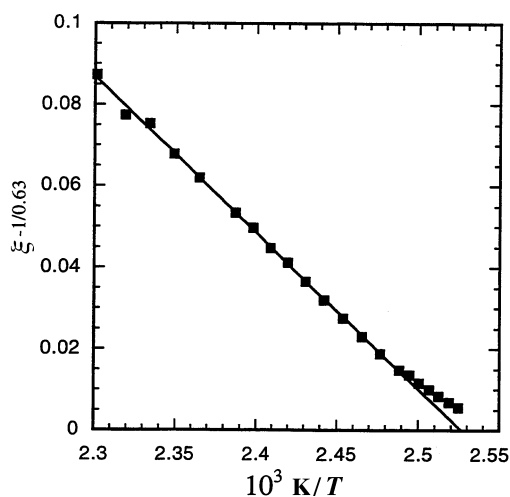


**Fig. 7** Dynamic correlation length  $\xi$  (in nm) raised to the power  $-1/0.63$  as a function of inverse temperature for the symmetric blend with  $\phi_H = 0.929$ . As the phase boundary is approached there are clear deviations from Ising behavior (the straight line fit).



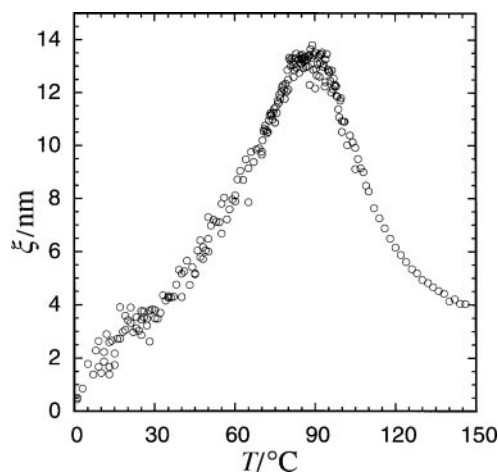


**Fig. 8** Dynamic correlation length  $\xi$  as a function of temperature for the symmetric blend with  $\phi_H = 0.900$ . Two phases are present: disordered at high temperature, and microemulsion at low temperature.

correlation length *via* eqn. (4) and the results are shown in Fig. 8. The results are clearly very different from the previous mixtures. Although at high temperatures  $\xi$  begins to increase strongly upon cooling, this trend is suddenly arrested near 90 °C, and from then on  $\xi$  decreases with decreasing  $T$ . The resulting maximum in  $\xi$  near 83 °C is clearly associated with the transition into the  $\mu$ E phase. This can be seen by examining  $S(q)$  from SANS for this sample, as a function of  $T$ , presented in Fig. 9. The characteristic feature of the  $\mu$ E is the appearance of a peak in  $S(q)$ , reminiscent of the transition from  $q^* = 0$  to  $q^* > 0$  at the LP anticipated by mean-field theory. This peak first appears between 70 and 80 °C. An expression for  $S(q)$  in the  $\mu$ E phase has been proposed by Teubner and Strey:<sup>46</sup>

$$S(q) \sim \frac{1}{a_2 + c_1 q^2 + c_2 q^4} \quad (5)$$

where the coefficients are the same as in eqn. (2). This function exhibits a maximum when  $c_1 < 0$ , with the high  $q$  side of the peak decaying as  $q^{-4}$ . The curves in Fig. 9 can be fitted to eqn. (5), and

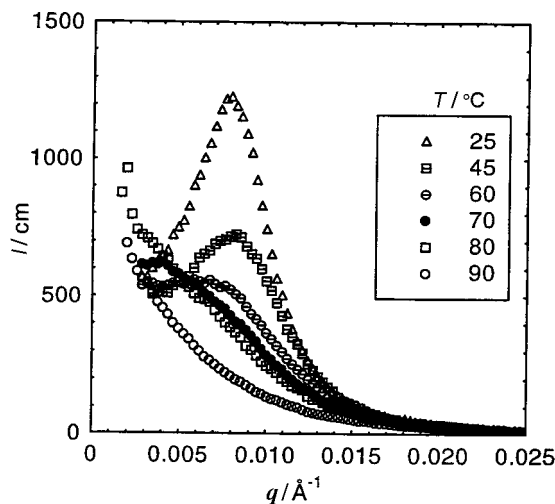


**Fig. 9** Scattered intensity as a function of scattering vector,  $q$ , as measured by SANS for the  $\phi_H = 0.900$  blend at the indicated temperatures. The emergence of a peak at finite  $q$  between 70 and 80 °C indicates the onset of the microemulsion phase.

the data are well described in this manner, as illustrated in Fig. 10 for the data at 25 °C. The resulting values of the coefficients as a function of temperature are shown in Fig. 11. The important result is that  $c_1$  changes sign at 72 °C, thereby crossing the Lifshitz line,<sup>9</sup> which may be taken as the transition into the  $\mu$ E phase. This temperature is slightly lower than the temperature, 83 °C, at which  $\xi$  from DLS exhibits a maximum. This may indicate that whereas the change in sign of  $c_1$  corresponds to the temperature at which the presence of interface begins to lower the free energy, the onset of the effect of interface in the dynamics may correspond more closely to where the  $c_1$  term is of order  $kT$ . Nevertheless, the SANS and DLS results are in good agreement as to the change in the nature of the material upon cooling from the fully disordered state.

The Teubner–Strey expression incorporates two length scales, a correlation length,  $\xi_{\text{TS}}$ , and a domain size (associated with the peak position),  $d$ .<sup>46</sup>

$$\xi_{\text{TS}} = \left[ \frac{1}{2} \left( \frac{a_2}{c_2} \right)^{1/2} + \frac{1}{4} \left( \frac{c_1}{c_2} \right) \right]^{-1/2} \quad (6a)$$

$$d = 2\pi \left[ \frac{1}{2} \left( \frac{a_2}{c_2} \right)^{1/2} - \frac{1}{4} \left( \frac{c_1}{c_2} \right) \right]^{-1/2} \quad (6b)$$

Accordingly, we can plot  $\xi_{\text{TS}}$  and  $d$  (divided by  $2\pi$  for convenience) along with  $\xi$  from DLS, as a function of  $T$  (Fig. 12). The results are quite interesting. Above 72 °C, where  $c_1 > 0$ ,  $\xi$  and  $\xi_{\text{TS}}$  are essentially the same, as expected for an Ornstein–Zernicke-like structure factor. However, below this temperature they diverge, with  $\xi_{\text{TS}}$  increasing and  $\xi$  decreasing upon cooling. This reflects the fundamentally different nature of these two length-scales; the  $\mu$ E structure apparently accelerates the rate of collective diffusion considerably. Note, however, that the application of eqn. (4) to the  $\mu$ E phase is without explicit justification at this point. The periodicity  $d$  is larger than  $\xi_{\text{TS}}$  by a factor of about 3–4, which is roughly consistent with the results for oil/water surfactant systems,<sup>46</sup> and does not vary much with  $T$  once the peak in  $S(q)$  is well-developed.

Teubner and Strey also anticipate the effect of the structure on the collective diffusion, *i.e.*,

$$D(q) = D_0 \left( 1 + \frac{c_1}{a_2} q^2 + \frac{c_2}{a_2} q^4 \right) \quad (7)$$

following eqn. (3).<sup>46</sup> This indicates that  $\Gamma/q^2$  should develop a  $q$  dependence. Accordingly, in Fig. 13 we plot  $\Gamma$  versus  $q^2$  (actually  $\sin^2\theta/2$ ) at three different temperatures, 100, 50, and 25 °C. At the highest temperature,  $\Gamma$  versus  $q^2$  is clearly linear with zero intercept, but by 50 °C, significant curvature is apparent.

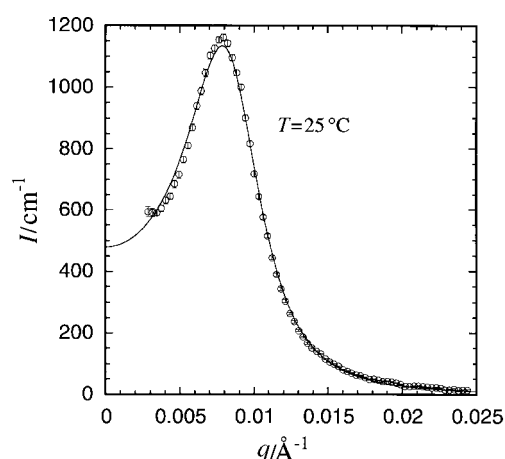


**Fig. 10** Scattered intensity as a function of scattering vector,  $q$ , as measured by SANS for the  $\phi_{\text{H}} = 0.900$  blend at 25 °C. The curve is a fit to the model by Teubner and Strey [eqn. (5)].<sup>46</sup>

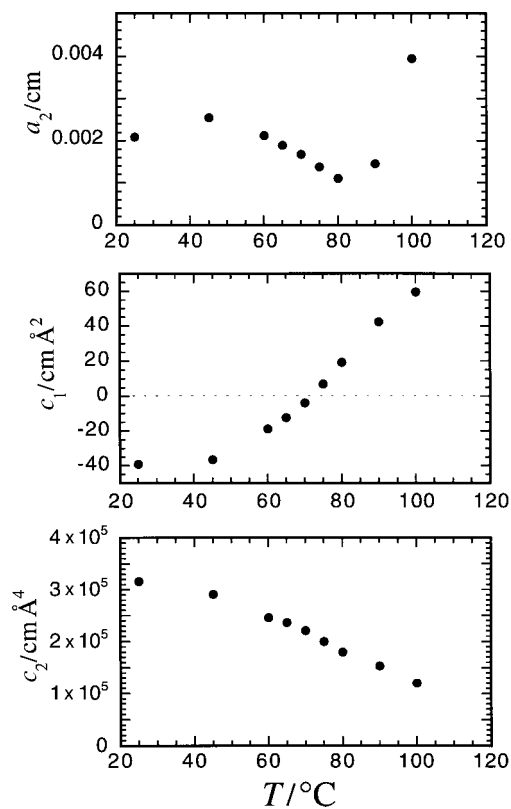


**Fig. 11** Coefficients of the Teubner–Strey model,<sup>46</sup>  $a_2$ ,  $c_1$ , and  $c_2$ , plotted as a function of temperature, obtained from fits to the SANS measurements of the  $\phi_H = 0.900$  blend.  $c_1$  changes sign at 72 °C, which can be taken as the boundary between the microemulsion and the disordered phase.

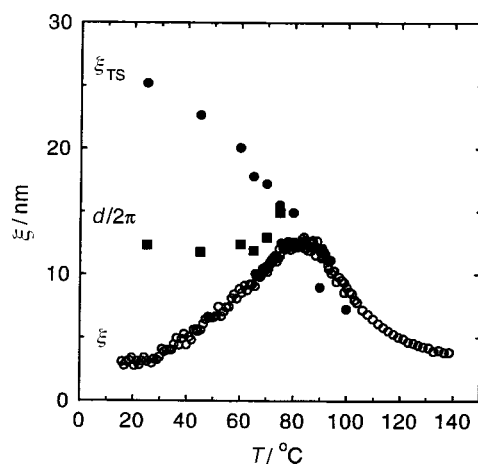


**Fig. 12** Static and dynamic length scales plotted as a function of temperature for the  $\phi_H = 0.900$  blend. The dynamic correlation length,  $\xi$ , is determined by DLS, whereas the static correlation length,  $\xi_{TS}$ , and the domain size,  $d$  (divided by  $2\pi$  for convenience), are obtained by SANS using the Teubner–Strey model.<sup>46</sup>

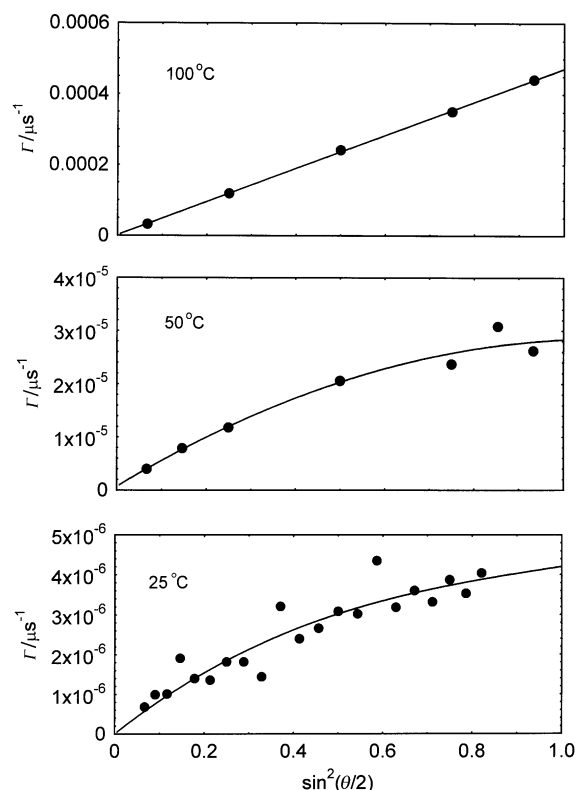


**Fig. 13** Angular dependence of the decay rate,  $\Gamma$ , for the  $\phi_H = 0.900$  blend at 100, 50, and 25 °C. At 100 °C, the blend is in the disordered phase, and the dynamics are purely diffusive, similar to the  $\phi_H = 1$  blend in the disordered phase. At lower temperatures, the decay rate develops an additional scattering vector dependence due to the effect of the microemulsion structure.

The Teubner–Strey fits, as illustrated in Fig. 10 and 11, provide the coefficients in order to compare eqn. (7) with the data. The fits in Fig. 13 exhibit a greater coefficient of  $q^2$  than given by the Teubner–Strey fits to  $S(q)$ , but follow the same trend of increasing with decreasing temperature.

As indicated previously, the correlation functions for the  $\phi_H = 0.900$  sample are dominated by a single diffusive mode, associated with  $\xi$ . More precisely, at temperatures above the maximum in  $\xi$ , the correlation functions are single exponential. Below the maximum, the correlation functions systematically include small amplitude, faster modes. An example is shown in Fig. 14, for a correlation function obtained at  $\theta = 90^\circ$  and  $T = 32^\circ\text{C}$ . In this case, two additional modes are resolved. As the amplitudes of these modes are always small, it is difficult to quantify their  $q$  dependence rigorously, but it appears to be diffusive. The physical processes to which the modes correspond are not immediately obvious, but presumably at least one involves the motion of the copolymer through homopolymer-rich regions, as suggested in the Background section. This behavior will be shown in the following section to be quite similar to the results for copolymer-rich samples in the LAM state.

A similar series of measurements was made for a sample with  $\phi_H = 0.908$ , *i.e.*, slightly closer to the predicted  $\phi_{LP}$ . The results for  $\xi(T)$  are shown in Fig. 15. They are clearly very similar to those for the sample with  $\phi_H = 0.900$ , including the temperature of the maximum. This implies that the Lifshitz line is far from vertical on the phase diagram; this has also been noted by Schwahn and coworkers.<sup>2</sup> The maximum value of  $\xi$  is greater in the  $\phi_H = 0.908$  sample, presumably because the smaller amount of copolymer allows the concentration fluctuations to grow further in spatial extent before the  $\mu\text{E}$  intervenes. The detailed analysis of the correlation functions is also similar: a single diffusive mode at high  $T$ , and additional small amplitude faster modes at low  $T$ . There is

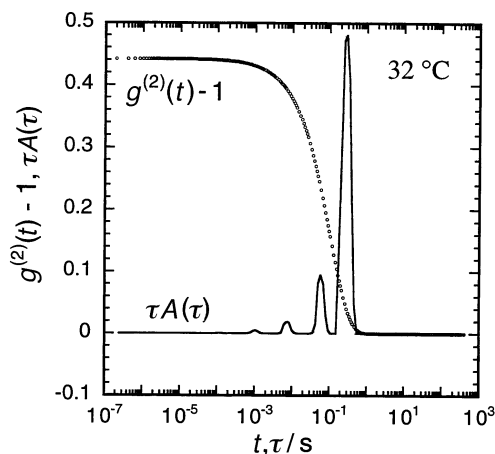


**Fig. 14** Intensity correlation functions,  $g^{(2)}(t)$ , for the  $\phi_H = 0.900$  blend measured at  $T = 32^\circ\text{C}$  and angle  $\theta = 90^\circ$ . The smooth curve indicates the corresponding distribution of decay times determined by inverse Laplace transformation. In addition to the main mode, attributed to monomer concentration fluctuations, at least two faster modes are resolved.

one new feature, however; a gap in the data emerges between about  $35$  and  $65^\circ\text{C}$ , over which interval the sample apparently passes into the phase-separated regime. The evidence for this is that the scattered intensity dropped abruptly both upon cooling below  $70^\circ\text{C}$  or upon heating above  $35^\circ\text{C}$ , due to an increase in turbidity. The corresponding  $\xi$  also dropped, due to an increase in  $\Gamma$ . TEM measurements on a similar system, PE/PEP, indicate a complementary droplet microemulsion structure in the phase-separated regime (see Fig. 3),<sup>5,45</sup> which would be consistent with an increased turbidity, due to a coarser structure, and also to the absence of formation of macroscopic phases, due to the small driving force for coarsening the local droplet microemulsions. The interesting feature of this sample, therefore, is the “re-entrant”  $\mu\text{E}$  phase, which exhibits behavior both above and below the phase-separated window entirely consistent with the  $0.900$  sample.

#### Copolymer-rich blends

On this side of the phase diagram we have examined one sample, with  $\phi_H = 0.820$ , and to some extent the pure diblock. However, in a previous report we described extensive DLS measurements

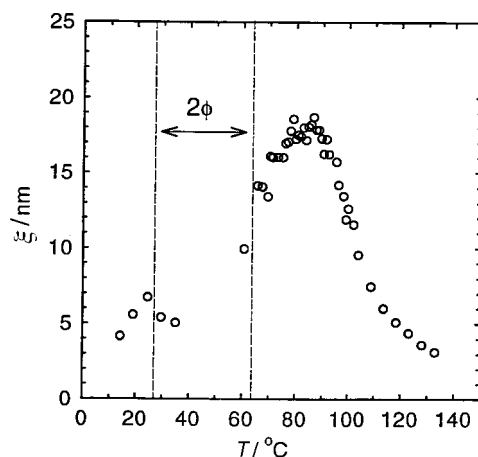


**Fig. 15** Dynamic correlation length  $\xi$  as a function of temperature for the symmetric blend with  $\phi_H = 0.908$ . In this blend, the phases are: disordered above  $86^\circ\text{C}$ , microemulsion from  $86$  to  $70^\circ\text{C}$ , phase-separated from  $65$  to  $35^\circ\text{C}$ , and finally, a “re-entrant” microemulsion phase below  $35^\circ\text{C}$ .

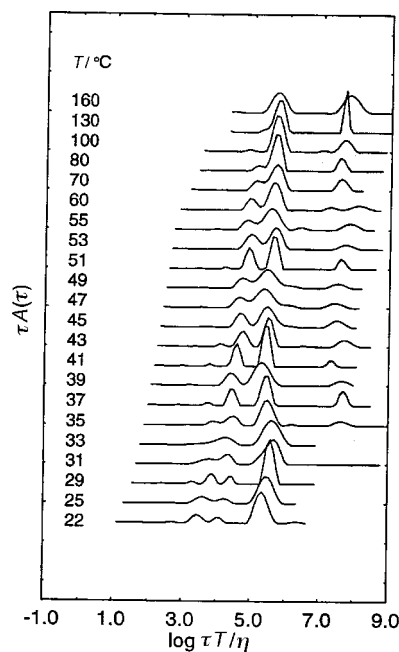


**Fig. 16** Distribution of normalized decay times as a function of reduced decay time,  $\tau\eta/T$ , for the  $\phi_H = 0.820$  blend at the indicated temperatures. The main mode is diffusive but is independent of the normalized decay time.

on a PDMS–PEP diblock of similar weight, which serves as a reference.<sup>16</sup> In that sample three modes were consistently resolved. The slowest, which has the largest amplitude, is the so-called “cluster mode” that appears in most block copolymer and homopolymer melts studied by DLS, and is of no particular interest in the current context. The intermediate mode was diffusive, and reasonably consistent with the expected copolymer mobility, and was thus assigned to the “heterogeneity” mode discussed in the Background section. The fastest mode was also diffusive, and its origins were less clear, although the diffusion of adventitious homopolymer in the sample is one possibility. Another, more interesting possibility is the undulation mode predicted<sup>47</sup> and reported<sup>48</sup> for swollen layered phases.

The REPES inversions of the correlation functions obtained from the  $\phi_H = 0.820$  sample are shown in Fig. 16. The horizontal axis is  $\tau$  ( $=1/I$ ) normalized by  $T/\eta$ , to remove the temperature dependence of the viscosity. The ODT is located at 36 °C. As many as four modes are resolved. The very slowest mode has all the characteristics of the “cluster” mode. The largest amplitude mode is diffusive, and attributable to the long wavelength concentration fluctuations that are not possible in the pure block copolymer. There is thus a correlation length associated with this mode, but the fact that this peak is almost independent of  $\tau T/\eta$  implies that  $\xi$  ( $\approx 2 \pm 1$  nm) does not vary much with  $T$ , in marked contrast to the  $\mu\text{E}$  case. This is true even below the ODT. There is a slightly faster, diffusive mode clearly resolvable below 80 °C that is consistent with the heterogeneity mode, and a still faster mode appearing in the ordered state, possibly the undulation mode. In short, the correlation functions in the ordered LAM state are very similar in character to those in the  $\mu\text{E}$  phase at low temperatures, although the  $T$  dependence of  $\xi$  is different. This is eminently reasonable, in that the structural distinctions between a highly homopolymer-swollen fluctuating LAM state and a bicontinuous  $\mu\text{E}$  should not be very great.

## Summary

The dynamic light scattering properties of model symmetric ternary polymer blends have been examined, particularly in and near the bicontinuous microemulsion channel on the space diagram.

Emphasis is placed on the temperature dependence of the dynamic correlation length,  $\xi$ , which is obtained from the decay rate of concentration fluctuations *via* the Kawasaki–Stokes–Einstein equation. In a binary homopolymer blend,  $\xi$  exhibits critical slowing down consistent with the Ising universality class. Addition of small amounts of copolymer depresses the critical temperature and modifies the critical exponent. For a narrow range of copolymer compositions, near where mean-field theory anticipates an isotropic Lifshitz point,  $\xi(T)$  exhibits a distinct maximum. At high temperatures,  $\xi$  increases as though approaching phase separation. However, near the temperature where the static structure factor first exhibits a peak at finite wavevector  $q^*$ , *i.e.*, the Lifshitz line,  $\xi$  begins to decrease with further cooling. One composition actually exhibits a re-entrant microemulsion phase, as the sample passes into the phase-separated region and then back into the microemulsion channel upon cooling. In the microemulsion phase, and also in the swollen lamellar phase at higher copolymer concentrations, the intensity autocorrelation functions include small amplitude, faster components attributable to copolymer diffusion and/or undulation of the copolymer-laden interfaces.

## Acknowledgements

This work was supported in part by the National Science Foundation, through awards DMR-9405101 (FSB) and DMT-9528481 (TPL), by NATO, through a Collaborative Research Grant (TPL and PS), by the Grant Agency of the Academy of Sciences of the Czech Republic through award A1050902 (PS), and by the Center for Interfacial Engineering, an NSF-sponsored Engineering Research Center at the University of Minnesota. Marc Hillmyer contributed helpful suggestions on both the measurements and the manuscript.

## References

- 1 H. S. Jeon, J. H. Lee and N. P. Balsara, *Phys. Rev. Lett.*, 1997, **79**, 3274.
- 2 D. Schwahn, K. Mortensen, H. Frielinghaus and K. Almdal, *Phys. Rev. Lett.*, 1999, **82**, 5056.
- 3 A. Adedeji, A. M. Jamieson and S. D. Hudson, *Macromolecules*, 1994, **27**, 4018.
- 4 B. Lowenhaupt, A. Steurer, G. P. Hellmann and Y. Gallot, *Macromolecules*, 1994, **27**, 908.
- 5 F. S. Bates, W. W. Maurer, P. M. Lipic, M. A. Hillmyer, K. Almdal, K. Mortensen, G. H. Fredrickson and T. P. Lodge, *Phys. Rev. Lett.*, 1997, **79**, 849.
- 6 F. S. Bates, *Science*, 1991, **251**, 898.
- 7 M. A. Hillmyer, K. Almdal, T. P. Lodge, W. W. Maurer and F. S. Bates, *J. Phys. Chem. B*, 1999, in the press.
- 8 D. Broseta and G. H. Fredrickson, *J. Chem. Phys.*, 1990, **93**, 2927.
- 9 R. Holyst and M. Schick, *J. Chem. Phys.*, 1992, **96**, 7728.
- 10 R. M. Hornreich, M. Luban and S. Shtrikman, *Phys. Rev. Lett.*, 1975, **35**, 1678.
- 11 F. S. Bates, W. W. Maurer, T. P. Lodge, M. F. Schulz, M. W. Matsen, K. Almdal and K. Mortensen, *Phys. Rev. Lett.*, 1995, **75**, 4429.
- 12 M. Kahlweit, R. Strey, D. Haase, H. Kunieda, T. Schmeling, B. Faulhaber, M. Borkovec, H.-F. Eicke, G. Busse, F. Eggers, T. Funck, H. Richmann, L. Magid, O. Söderman, P. Stilbs, J. Winkler, A. Dittrich and W. Jahn, *J. Colloid Interface Sci.*, 1987, **118**, 436.
- 13 I. Musevic, B. Zeks, R. Blinc, M. M. Wittebrood and T. Rasing, *Physica B*, 1995, **211**, 331.
- 14 I. Musevic, A. Rastegar, M. Cepic, B. Zeks, M. Copic, D. Moro and G. Heppke, *Phys. Rev. Lett.*, 1996, **77**, 1769.
- 15 K. Almdal, M. A. Hillmyer and F. S. Bates, *Macromolecules*, 1999, in the press.
- 16 P. Stepanek, K. Almdal and T. P. Lodge, *J. Polym. Sci., Polym. Phys. Ed.*, 1997, **35**, 1643.
- 17 P. Stepanek, T. P. Lodge, C. Kedrowski and F. S. Bates, *J. Chem. Phys.*, 1991, **94**, 8289.
- 18 J. Jakes, *Collect. Czech. Chem. Commun.*, 1995, **60**, 1781.
- 19 J. Jakes, *Czech. J. Phys.*, 1988, **38**, 1305.
- 20 S. W. Provencher, *Comput. Phys. Commun.*, 1982, **27**, 229.
- 21 J. D. Ferry, *Viscoelastic Properties of Polymers*, Wiley, New York, 3rd edn., 1980.
- 22 M. Banaszak and M. D. Whitmore, *Macromolecules*, 1992, **25**, 249.
- 23 P. K. Janert and M. Schick, *Macromolecules*, 1997, **30**, 3916.
- 24 P. K. Janert and M. Schick, *Macromolecules*, 1997, **30**, 137.
- 25 D. Schwahn, K. Mortensen and H. Yee-Madeira, *Phys. Rev. Lett.*, 1987, **58**, 1544.
- 26 D. Schwahn, G. Meier, K. Mortensen and S. Janssen, *J. Phys. II*, 1994, **4**, 837.
- 27 G. Meier, B. Momper and E. W. Fischer, *J. Chem. Phys.*, 1992, **97**, 5884.



- 28 F. S. Bates, J. H. Rosedale, P. Stepanek, T. P. Lodge, P. Wiltzius, G. H. Fredrickson and R. P. Hjelm, *Phys. Rev. Lett.*, 1990, **65**, 1893.
- 29 K. Binder, *Adv. Polym. Sci.*, 1994, **112**, 181.
- 30 P.-G. de Gennes, *J. Phys. Lett.*, 1977, **38**, L-441.
- 31 J. F. Joanny, *J. Phys. A*, 1978, **11**, L117.
- 32 S. A. Brazovskii, *Sov. Phys. JETP (Engl. Transl.)*, 1975, **41**, 85.
- 33 L. Leibler, *Macromolecules*, 1980, **13**, 1602.
- 34 G. H. Fredrickson and E. Helfand, *J. Chem. Phys.*, 1987, **87**, 697.
- 35 W. W. Maurer, F. S. Bates, T. P. Lodge, K. Almdal, K. Mortensen and G. H. Fredrickson, *J. Chem. Phys.*, 1998, **108**, 2989.
- 36 G. H. Fredrickson and F. S. Bates, *J. Polym. Sci., Polym. Phys. Ed.*, 1997, **35**, 2775.
- 37 M. Benmouna, H. Benoit, M. Duval and A. Z. Akcasu, *Macromolecules*, 1987, **20**, 1107.
- 38 M. Benmouna, H. Benoit, R. Borsali and M. Duval, *Macromolecules*, 1987, **20**, 2620.
- 39 A. Z. Akcasu, G. Nägele and R. Klein, *Macromolecules*, 1991, **24**, 4408.
- 40 A. Z. Akcasu and M. Tombakoglu, *Macromolecules*, 1990, **23**, 607.
- 41 T. Jian, S. H. Anastasiadis, A. N. Semenov, G. Fytas, K. Adachi and T. Kotaka, *Macromolecules*, 1994, **27**, 4762.
- 42 M. Benmouna, M. Duval and R. Borsali, *J. Polym. Sci., Polym. Phys. Ed.*, 1987, **25**, 1839.
- 43 C. Pan, W. Maurer, Z. Liu, T. P. Lodge, P. Stepanek, E. D. von Meerwall and H. Watanabe, *Macromolecules*, 1995, **28**, 1643.
- 44 P. Stepanek and T. P. Lodge, *Macromolecules*, 1996, **29**, 1244.
- 45 W. W. Maurer, PhD Thesis, University of Minnesota, Minneapolis, MN, 1998.
- 46 M. Teubner and R. Strey, *J. Chem. Phys.*, 1987, **87**, 3195.
- 47 P. G. de Gennes, *J. Phys. (Paris)*, 1969, **30**, C4–65.
- 48 R. Ribotta, D. Salin and G. Durand, *Phys. Rev. Lett.*, 1974, **32**, 6.

Paper 8/09169B